ELSEVIER

Journal of Alloys and Compounds 404–406 (2005) 238–242

Journal of ALLOYS AND COMPOUNDS

www.elsevier.com/locate/jallcom

^{1}H NMR analysis of nuclear relaxation mechanisms in Pd–H and Pd–Ag–H alloys

M. Bokor*, P. Bánki, G. Lasanda, K. Tompa

Research Institute for Solid State Physics and Optics of the Hungarian Academy of Sciences, Konkoly-Thege út 29-33, 1121 Budapest, Hungary

Received 31 May 2004; received in revised form 22 December 2004; accepted 5 January 2005
Available online 7 July 2005

Abstract

Crystalline $Pd_{1-x}Ag_x$–H_y ($x = 0$–0.35) alloys were studied as model systems representing a chemically disordered system for hydrogen-storage materials. Extensive ^{1}H relaxation rate (R_1, $R_{1\rho}$ and R_2) measurements were carried out in a wide temperature range of 2.4–400 K. Palladium–silver alloys of silver concentration as high as 35 at.% were studied by NMR spectroscopy for the first time. The relaxation mechanisms magnetic dipolar relaxation (hydrogen diffusion), Korringa relaxation, relaxation by paramagnetic impurity ions and cross-relaxation to quadrupolar metal nuclei were identified and characterized. The presence of cross-relaxation between ^{1}H and quadrupolar ^{105}Pd nuclear spins was assumed and demonstrated for the first time in Pd–H and $Pd_{1-x}Ag_x$–H systems. More than one jump processes of diffusing hydrogen were found to be present in the studied palladium–silver alloys. Only lower estimated limit values of Korringa constants could be obtained since no frequency independent R_1 versus T region was found. These values are significantly higher than the ones reported by others.

Keywords: Disordered systems; Hydrogen-storage materials; Nuclear resonances

1. Introduction

Proton spin–lattice-relaxation rates R_1 are often used in nuclear magnetic resonance (NMR) studies of electronic structure and hydrogen motion in metal–hydrogen systems. The total spin–lattice-relaxation rate is usually taken to be the sum of three terms [1]: R_{1d} is due to dipole–dipole interaction modulated by hydrogen diffusion, R_{1e} is the electronic (Korringa) relaxation rate, and R_{1p} represents relaxation due to paramagnetic impurities. In our case, there should be included the effects of yet another spin–lattice relaxation mechanism, R_{1c}, in which protons cross relax with quadrupolar metal nuclei, which in turn transfer energy to the lattice via their own relaxation rates [2]: $R_1 = R_{1d} + R_{1e} + R_{1p} + R_{1c}$.

* Corresponding author. Tel.: +36 13922795; fax: +36 13922215.
E-mail address: mbokor@szfki.hu (M. Bokor).

0925-8388/$ – see front matter © 2005 Elsevier B.V. All rights reserved.
doi:10.1016/j.jallcom.2005.01.117

2. Nuclear relaxation mechanisms

2.1. Hydrogen diffusion

The spectral density functions relevant to nuclear spin relaxation due to dipolar coupling between diffusing ^{1}H spins in an fcc lattice (intrinsic diffusion, simple hopping model) were calculated numerically by Monte Carlo method [3]. A new analytic form for the spectral densities was introduced by Sholl [4] which adequately represents the results of the numerical calculations. The relaxation rates for a polycrystalline sample are described by the formulae:

$$R_1 = Ay_0(g(y_0) + 4g(2y_0)), \tag{1}$$

$$R_{1\rho} = \frac{A}{2}y_0(3g(2y_1) + 5g(y_0) + 2g(2y_0)) \tag{2}$$

and

$$R_2 = \frac{A}{2}y_0(3g(0) + 5g(y_0) + 2g(2y_0)), \tag{3}$$

where $A = (\mu_0/4\pi)^2 2\gamma^4\hbar^2 I(I+1)c/(5a^6\omega_0)$ and γ is the nuclear gyromagnetic ratio, I is the nuclear spin, c is the fraction of sites occupied by spins, a is the lattice parameter, ω_0 is the Larmor frequency and $y_i = \omega_i\tau/2$. The mean time between jumps of a spin is $\tau = \tau_0 \exp(E/RT)$. The analytic form for $g(y)$ is $g(y) = S/(a_1 + a_2 y^{1/2} + a_3 y^u + a_4 y^v + y^2)$, where the parameters S, a_i, u and v are chosen to fit the numerical results.

2.2. Korringa relaxation

The interaction between protons and conduction electrons manifests in a field-independent relaxation term—the Korringa relaxation described as $R_{1e} = R_{1\rho e} = R_{2e} = T/\kappa$. The constant κ is inversely proportional to the electron density of states at the Fermi level.

2.3. Relaxation due to paramagnetic impurities

Low levels of paramagnetic impurities (10–100 ppm) can have profound effects on the spin–lattice relaxation rate [5]: they produce considerably more asymmetric maxima than the theories predict in the temperature dependence of the proton R_{1d}, with a shallower low-temperature slope or secondary maxima on the low-temperature side of the maximum. There are two important mechanisms for the transport of the excess energy in the nuclear spin system. Proton magnetization is transported to the paramagnetic ions (relaxation centers) by spin diffusion when hydrogen motion is frozen at low temperatures and by atomic diffusion at intermediate and high temperatures.

2.4. Cross-relaxation between ^{1}H and quadrupolar nuclear spins

Proton spin–lattice relaxation rates R_1 reveal an anomalous frequency dependence in several metal–hydrogen systems [1,2,6] at $T < 100$ K. In addition, many of the ^{1}H R_1 data have weaker than linear temperature dependencies. Both observations are unusual since Korringa relaxation [7] is expected what predicts relaxation rates linear in temperature and independent of resonance frequency. Absorbed hydrogen and silver alloying destroys the ideal cubic symmetry of the palladium lattice in $Pd_{1x}Ag_x$–H_y samples. There is thus a distribution of electric field gradients (EFG) at quadrupolar ^{105}Pd nuclei, as well as of orientations of the EFG axes with respect to the applied field B_0. Cross-relaxation due to dipolar interaction between the two spin systems (R_{1cr}) can occur when the Zeeman energy splitting of an ^{1}H spin happens to equal some combined Zeeman-quadrupolar splitting of a nearby ^{105}Pd nuclear spin. The spin energy is transferred from the ^{1}H spin system (I) to that of the quadrupolar ^{105}Pd nuclei (S) (R_{1cr} term) and then on to the lattice (R_{1S} term) to give an overall relaxation rate R_{1c} [2]. At temperatures at which hydrogen diffusion occurs, R_{1cr} is progressively removed—averaged by the motion. If hydrogen diffusion is absent, R_{1cr} is independent of temperature unless a structural phase change occurs. If R_{1S} is fast enough not to constitute a bottleneck then R_{1c} is also temperature independent. Since the Zeeman energies depend on B_0, the cross-relaxation rate R_{1cr} will likewise vary with field (^{1}H NMR frequency). In most materials studied to date [2,6] R_{1S} has been fast enough to maintain a common spin temperature between the lattice and the S-spin system. In such cases R_{1S} plays a negligible role since the temperature and frequency dependences of R_{1c} are then determined solely by R_{1cr} which is basically independent of temperature in rigid solids.

3. Experimental

Twenty-five micrometre thick palladium foil of 99.95% purity was purchased from Goodfellow. For the alloys, lumps of palladium (99.95%) and silver (99.99%) were mixed and alloyed by induction melting under reduced argon pressure of 8×10^4 Pa. To reach homogeneity, the ingots were remelted three times. The alloys were cold rolled in five to seven steps to a thickness of 20 μm. The steps of cold rolling were separated by surface cleaning in 6 M hydrochloric acid and annealing at 973 K. The samples was charged with hydrogen to the maximum available metal to hydrogen atomic ratio (Table 1) from the gas phase at atmospheric pressure at 373 K. According to the manufacturers data, iron is the only impurity of magnetic nature in the starting materials. The nominal iron impurity concentrations were 19 ppm for Pd, 18 ppm for $Pd_{0.90}Ag_{0.10}$, 16 ppm for $Pd_{0.80}Ag_{0.20}$ and 14 ppm for $Pd_{0.65}Ag_{0.35}$ as calculated from manufacturers data of 10 wt. ppm Fe in Pd and 2 wt. ppm Fe in Ag.

^{1}H NMR measurements and data acquisition were accomplished by a Bruker SXP 4-100. Stability of magnetic field and frequency was better than $\pm 10^{-6}$. Temperature was controlled by an open-cycle Oxford cryostat with an uncertainty less than ±1 K. Spin–lattice relaxation rates R_1 were measured by inversion-recovery method. Rotating-frame rates $R_{1\rho}$ were obtained by applying a 90° pulse, immediately followed by a long spin-locking pulse, phase shifted by 90° with respect to 90° pulse. Spin–spin relaxation rates R_2 were measured by CPMG method with a delay time $2\tau = 0.1$ ms.

4. Results and discussion

No field-independent R_1 versus T region could be found for the metal hydrides investigated (Fig. 1). A linear-fit approach was applied to determine constant κ. This method is based on the assumption that in the rigid-lattice regime where $R_1 = R_{1e} + R_{1p} + R_{1c}$ the relaxation rate R_{1p} is constant and independent of temperature [5]. The constant κ was then determined from the slope of the line fitted to the R_1 versus T data measured at $T < 50$ K (Fig. 2 and Table 1). The field dependent intercepts of the straight lines on the R_1 axis

Table 1
Parameter values obtained by the analysis of the temperature and frequency dependences of ^{1}H R_1 and $R_{1\rho}$ data (bold numbers) measured in $Pd_{1x}Ag_x$–H_y alloys

	x			
	0	0.10	0.20	0.35
y	0.61–0.78	0.55–0.59	0.45	0.27
κ (sK)	**110**; 68–70 [13]	**118**; 62±2.5 [14][b]	**121**	**106**
$R_1(T = 0\,K)$[c] (s^{-1})	**0.62**; **0.31**	**0.28**; **0.14**	**0.08**; **0.04**	**0.17**; **0.08**
E (kJ/mol)	**22.2**[a]; 22.2 [15]	**23.8**[d]; 23 [10][e], 24 [16]	**24.4**; 28.5 [17]	**27.9**
τ_0 (10^{-13} s)	**0.91**; 1.3 [18]	**0.86**[d]; 0.88 [10][e]	**2.0**	**1.3**
D_0 (10^{-7} m^2/s)	**1.6**	**1.7**	**0.72**	**1.2**
$\sqrt{\langle l^2\rangle}$ (nm)	**0.296**	**0.297**	**0.297**	**0.295**
$D_0/(1-c)$ (10^{-7} m^2/s)	**5.5**; 2.9 [15]	**4.1**; 3.9 [16]	**1.3**; 1.09 [17]	**1.6**
M_2 (10^{-8} T^2)	**5.0**; 4.9[f]	**4.4**[g]; 4.4[f]	**3.4**[g]; 3.4[f]	**2.1**[g]; 2.1[f]

Diffusion constants D_0 were calculated as $\langle l^2\rangle/6\tau_0$ with the assumption $\sqrt{\langle l^2\rangle} = a$. The relevant results obtained by others are given for comparison (second columns), where available. The last significant figure of each value given is considered reliable to ±1, the estimated error of κ is 5%.

[a] Not varied, from [15].
[b] $Pd_{0.889}Ag_{0.111}$–H, from high-temperature R_1 data.
[c] From linear fit of the R_1 data measured at $T < 50$ K; $\nu_0 \approx 30$ and 90 MHz.
[d] Not varied, from the frequency dependence of the R_1 and $R_{1\rho}$ maxima.
[e] From temperature dependence of R_2 data.
[f] Calculated from spectra of ^{1}H free induction decay signals measured at $T = 2.4$ K.
[g] Not varied, from spectrum measurements (footnote f).

(Table 1) give the sum of the (constant) impurity rate R_{1p} and the field dependent cross-relaxation rate R_{1c}. The high-temperature sides of the R_1 and $R_{1\rho}$ maxima were interpreted as $R = R_d + R_e$ (Fig. 1). Eqs. (1) and (2) were fitted to the experimental R_1 and $R_{1\rho}$ data, the appropriate values of parameters S, a_i, u and v for fcc lattice were taken from [4]. The spin–spin relaxation rate curves calculated with the parameters of the R_1 and $R_{1\rho}$ fit (Eq. (3), dashed lines in Fig. 1) showed reasonable agreement with the measured points. The activation energy E of hydrogen diffusion shows the expected trend [8] of becoming larger with increasing silver content (Table 1). The 0.295–0.297 nm values of lattice parameter a resulting form the fit (Table 1, $\sqrt{\langle l^2\rangle} = a$) are close to the 0.285–0.286 nm distance between neighboring octahedral sites in $Pd_{1-x}Ag_x$–H_{max} alloys [9]. The second moment M_2 values calculated from spectra of ^{1}H free induction decay signals measured at $T = 2.4$ K decrease with increasing silver and diminishing hydrogen content. Experimental M_2 values resulted in relaxation rate maxima of right magnitudes.

The low-temperature sides of the R_1 and $R_{1\rho}$ maxima become more and more shallower than the high-temperature sides with increasing silver content. The presence of more

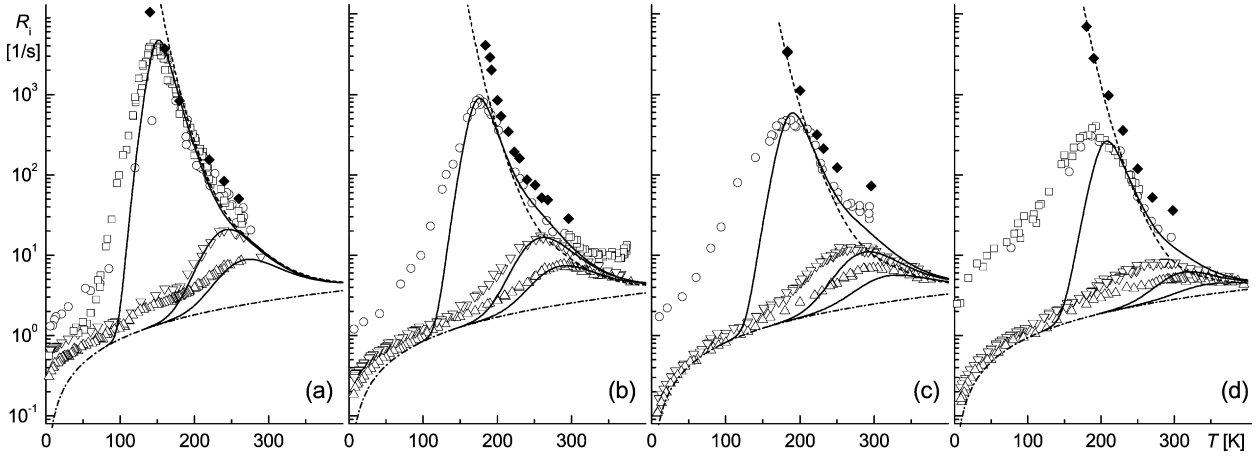

Fig. 1. ^{1}H relaxation rates R_1 (spin–lattice), $R_{1\rho}$ (rotating-frame spin–lattice) and R_2 (spin–spin) measured in $Pd_{1x}Ag_x$–H_{max} alloys. (a) Pd–H: triangles stand for R_1 at ν_0 = 28 and 83 MHz; $R_{1\rho}$ is denoted by circles (ν_0 = 28 MHz; ν_1 = 710 Hz) and by squares (ν_0 = 83 MHz; ν_1 = 170 Hz); diamonds are for R_2 (ν_0 = 83 MHz). (b) $Pd_{0.90}Ag_{0.10}$–H: triangles stand for R_1 at ν_0 = 28–30 and 87 MHz; $R_{1\rho}$ is denoted by circles (ν_0 = 28 MHz; ν_1 = 750 Hz) and by squares (ν_0 = 83 MHz; ν_1 = 330 Hz); diamonds are for R_2 (ν_0 = 87 MHz). (c) $Pd_{0.80}Ag_{0.20}$–H: triangles stand for R_1 at ν_0 = 28–30 and 87 MHz; $R_{1\rho}$ is denoted by circles (ν_0 = 28 MHz; ν_1 = 710 Hz); diamonds are for R_2 (ν_0 = 87 MHz). (d) $Pd_{0.65}Ag_{0.35}$–H: triangles stand for R_1 at ν_0 = 28–30 and 87 MHz; $R_{1\rho}$ is denoted by circles (ν_0 = 28 MHz; ν_1 = 750 Hz) and by squares (ν_0 = 28 MHz; ν_1 = 600 Hz); diamonds are for R_2 (ν_0 = 87 MHz). Lines are theoretical curves fitted (for details see text and Table 1). The Korringa relaxation contributions are shown by the dash-dotted lines. Spin–lattice relaxation rate curves are solid lines and the spin–spin relaxation rates are given by dashed lines.

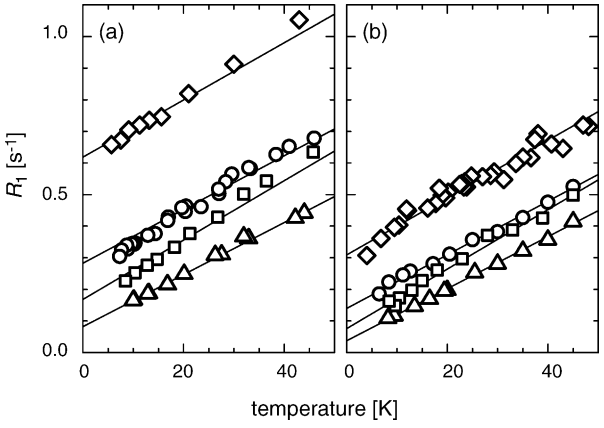

Fig. 2. Low-temperature ^{1}H spin–lattice relaxation rates R_1 for $Pd_{1x}Ag_x$–H_{max} alloys at (a) $\nu_0 = 28$ MHz and (b) $\nu_0 = 87$ MHz. Diamonds: Pd–H, circles: $Pd_{0.90}Ag_{0.10}$–H, triangles: $Pd_{0.80}Ag_{0.20}$–H and squares: $Pd_{0.65}Ag_{0.35}$–H. Linear fits: $R_1 = R_{1e} + R_{1p} + R_{1c}$, where R_{1p} and R_{1c} are temperature independent constants and $R_{1e} = T/\kappa$.

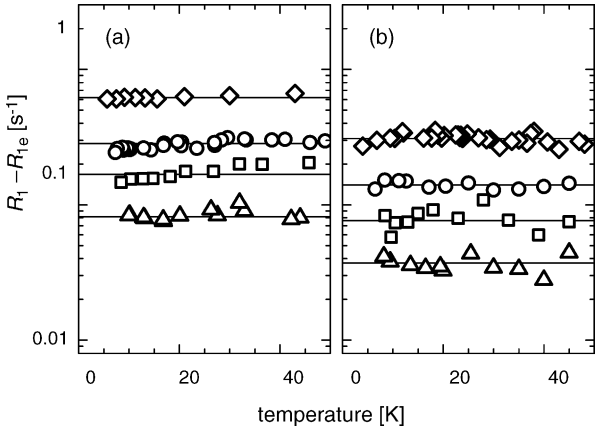

Fig. 3. Low-temperature ^{1}H spin–lattice relaxation rates without the electronic term ($R_1 - R_e$) for $Pd_{1x}Ag_x$–H_{max} alloys at (a) $\nu_0 = 28$ MHz and (b) $\nu_0 = 87$ MHz. Diamonds: Pd–H, circles: $Pd_{0.90}Ag_{0.10}$–H, triangles: $d_{0.80}Ag_{0.20}$–H and squares: $Pd_{0.65}Ag_{0.35}$–H.

than one jump processes of hydrogen diffusion can be made responsible for this feature mostly expressed when $x = 0.20$ and 0.35 (Fig. 1c and d). The measured R_2 data deviate from the calculated curves towards faster relaxation what points also to the existence of more than one jump processes.

Following the argumentation of [2], the mechanism of cross-relaxation between proton and quadrupolar ^{105}Pd nuclear spins was assumed to be mostly responsible for the observed deviations from the Korringa behavior, since $Pd_{1-x}Ag_x$–H_y systems (i) are of destroyed cubic symmetry (due to absorbed hydrogen and alloying with silver) and (ii) contain quadrupolar spins. This term is removed at higher temperatures, at which hydrogen diffusion occurs on the NMR frequency scale. At lower temperatures, where R_d is negligibly small, R_1 and $R_{1\rho}$ increased as the proton resonance frequency decreased. The relaxation rates after the subtraction of the electronic term are temperature independent at low T (R_1 below 100 K and $R_{1\rho}$ below 50 K; Fig. 3). This behavior suggests that R_{1S} is fast enough to maintain a common spin temperature between the lattice and the S-spin system. The temperature and frequency dependences of R_{1c} are then determined by R_{cr}, which is basically independent of temperature in rigid solids. Both paramagnetic relaxation and cross-relaxation are assumed to give a constant and temperature independent contribution to the ^{1}H spin–lattice relaxation rates at these very low temperatures of $T < 100$ K [5]. The $(R_1 - R_{1e})$ data are independent of temperature as expected (Fig. 3) and the paramagnetic and cross-relaxation mechanisms together determine their values. The extrapolated $R_1(T = 0\,K)$ values follow a decreasing trend with decreasing palladium content. The smaller value for $Pd_{0.80}Ag_{0.20}$ than for $Pd_{0.65}Ag_{0.35}$ is not yet understood but does not question the role of paramagnetic and cross-relaxation relaxations.

5. Conclusions

Extensive ^{1}H relaxation rate measurements were made on $Pd_{1-x}Ag_x$–H_y samples (Fig. 1). Only lower estimated limit values of Korringa constants could be obtained since no frequency independent R_1 and $R_{1\rho}$ versus T was found; these values are significantly higher than the ones reported by others. More than one jump processes of diffusing hydrogen were found in β-phase palladium–silver alloys of $x = 0.20$ and 0.35. Our earlier results on ^{1}H NMR spectrum shape ($x = 0.10$) [10] and spin–spin relaxation rate ($x = 0.25$) [11] support also this concept. Other authors have reported similar behavior only for α-phase $Pd_{0.9}Ag_{0.1}$–H and $Pd_{0.7}Ag_{0.3}$–H, these alloys show two and three jump processes, respectively [12]. Cross-relaxation between ^{1}H and quadrupolar ^{105}Pd nuclear spins was taken into account as a significant relaxation mechanism besides paramagnetic relaxation at low temperatures for the first time in the studied $Pd_{1-x}Ag_x$–H_y alloys.

Acknowledgements

This research was supported by Grants D38490, T31994 and TS040878 of the Hungarian Science Foundation (OTKA). M. Bokor is also indebted to the Hungarian Academy of Sciences for the Bolyai Scholarship.

References

[1] R.G. Barnes, Topics Appl. Phys. 73 (1997) 93–151.
[2] L.R. Lichty, J.-W. Han, D.R. Torgeson, R.G. Barnes, E.F.W. Seymour, Phys. Rev. B 42 (1990) 7734–7746.
[3] D.A. Faux, D.K. Ross, C.A. Sholl, J. Phys. C: Solid State Phys. 19 (1986) 4115–4133.
[4] C.A. Sholl, J. Phys. C: Solid State Phys. 21 (1988) 319–324.
[5] T.-T. Phua, B.J. Beaudry, D.T. Peterson, D.R. Torgeson, R.G. Barnes, M. Belhoul, G.A. Styles, E.F.W. Seymour, Phys. Rev. B 28 (1983) 6227–6250.

[6] D.B. Baker, M.S. Conradi, P.A. Fedders, R.E. Norberg, D.R. Torgeson, R.G. Barnes, Phys. Rev. B 44 (1991) 11759–11766.
[7] J. Korringa, Physica 16 (1950) 601–610.
[8] E. Salomons, H. Hemmes, R. Griessen, J. Phys.: Condens. Matter 2 (1990) 817–834.
[9] S.D. Axelrod, A.C. Makrides, J. Phys. Chem. 68 (1964) 2154–2159.
[10] K. Tompa, P. Bánki, M. Bokor, G. Lasanda, Europhys. Lett. 53 (2001) 79–85.
[11] K. Tompa, P. Bánki, M. Bokor, Defect Diff. Forum 224–225 (2003) 93–106.
[12] H. Züchner, H. Barlag, G. Majer, J. Alloys Compd. 330–332 (2002) 448–453.
[13] R.R. Arons, H.G. Bohn, H. Lütgemeier, Solid State Commun. 14 (1974) 1203–1205;
G.K. Schoep, N.J. Poulis, R.R. Arons, Physica 75 (1974) 297–304;
D.A. Cornell, E.F.W. Seymour, J. Less-Comm. Met. 39 (1975) 43–54.
[14] P.P. Davis, E.F.W. Seymour, J. Less-Comm. Met. 49 (1976) 159–168.
[15] G. Alefeld, J. Völkl (Eds.), Hydrogen in Metals, vols. I–II, Springer, Berlin, 1978.
[16] G. Holleck, E. Wicke, Z. Phys. Chem. NF 56 (1967) 155–159.
[17] G. Bohmholdt, E. Wicke, Z. Phys. Chem. NF 56 (1967) 133–137.
[18] D.A. Cornell, E.F.W. Seymour, J. Less-Comm. Met. 39 (1975) 43–54.